Different ion-qubit choises

- One electron in the valence shell; “Alkali like” $^2S_{1/2}$ ground state.

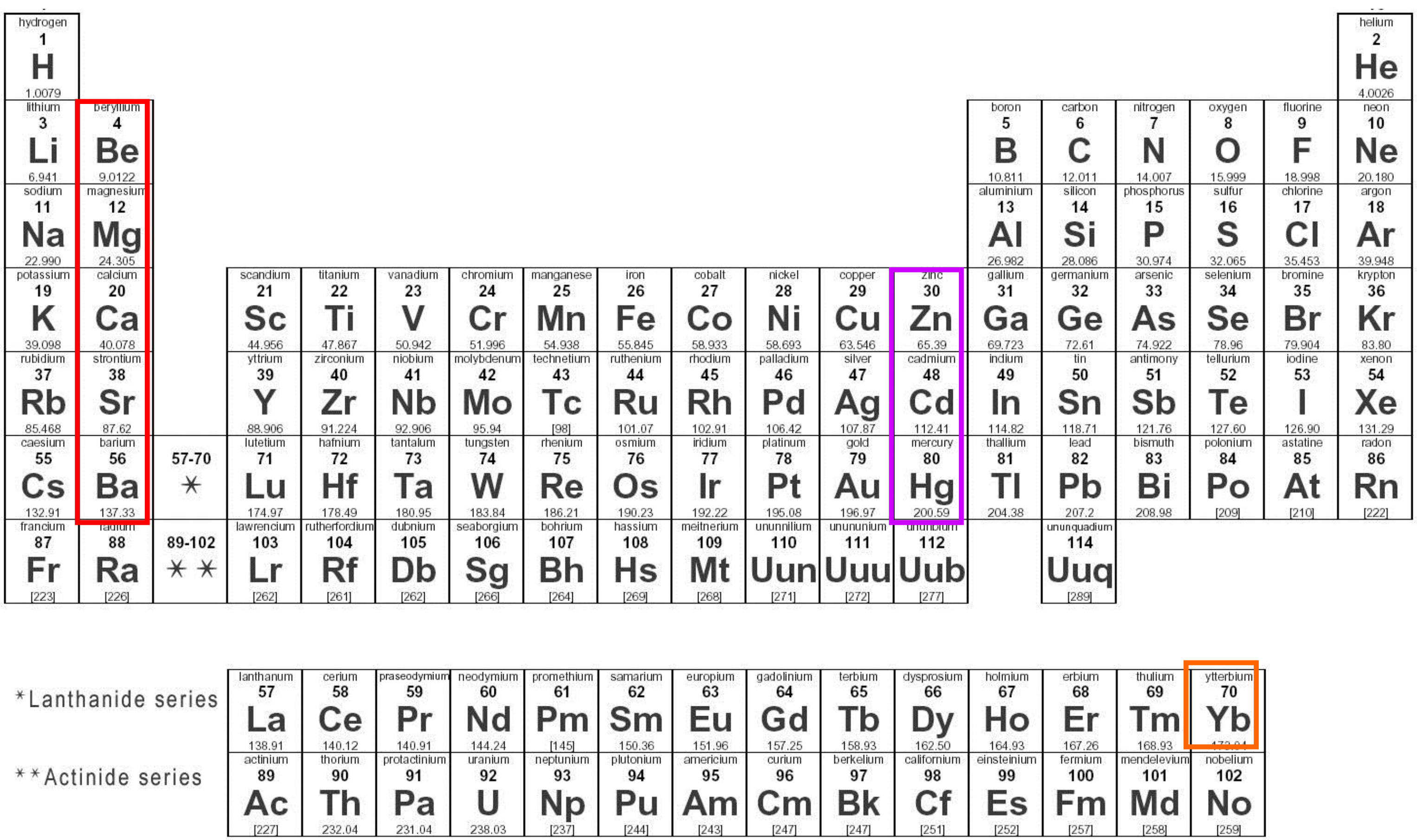

Electronic levels Structure

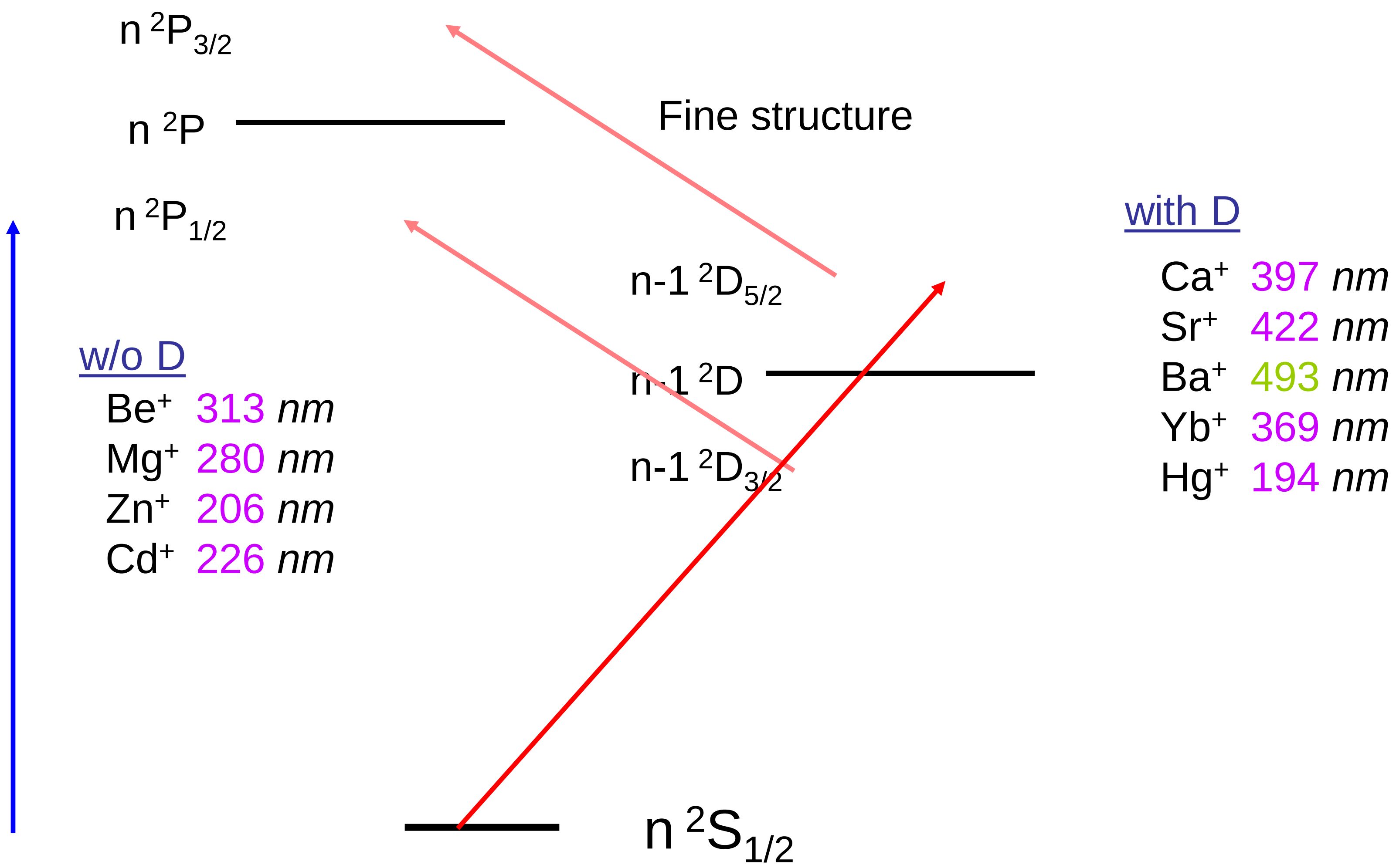

$^2S_{1/2}$ Zeeman qubit

(Isotopes w/o nuclear spin)

e.g.

- $^{24}Mg^+$
- $^{64}Zn^+$
- $^{114}Cd^+$
- $^{40}Ca+$
- $^{88}Sr+$
- $^{138}Ba+$
- $^{174}Yb+$
- $^{202}Hg+$

Advantages

- RF separation.
- Tunable.
- Infinite T_1.

Disadvantages

- Energy depends linearly on B.
- Transition photon caries no momentum
- Momentum transfer with off-resonance lasers: photon scattering.
- Detection.

m = 1/2 $|\uparrow\rangle$

n $^2S_{1/2}$

m = -1/2 $|\downarrow\rangle$

Turn on small B field
2.8 *MHz/G*

$^2S_{1/2}$ Hyperfine qubit

e.g.

$^9Be^+$
$^{25}Mg^+$
$^{67}Zn^+$
$^{111}Cd^+$
$^{43}Ca+$
$^{87}Sr+$
$^{137}Ba+$
$^{171}Yb+$
$^{199}Hg+$

Hyperfine structure (order depends on the sign of A_{hf})

Turn on small B field

Advantages

- MW energy separation.
- B-field independent qubit.
- Infinite T_1.
- State selective fluorescence Detection.

Disadvantages

- Few GHz energy separation.
- Transition photon caries no momentum
- Off resonance photon scattering.
- initialization to clock transition can be more tricky

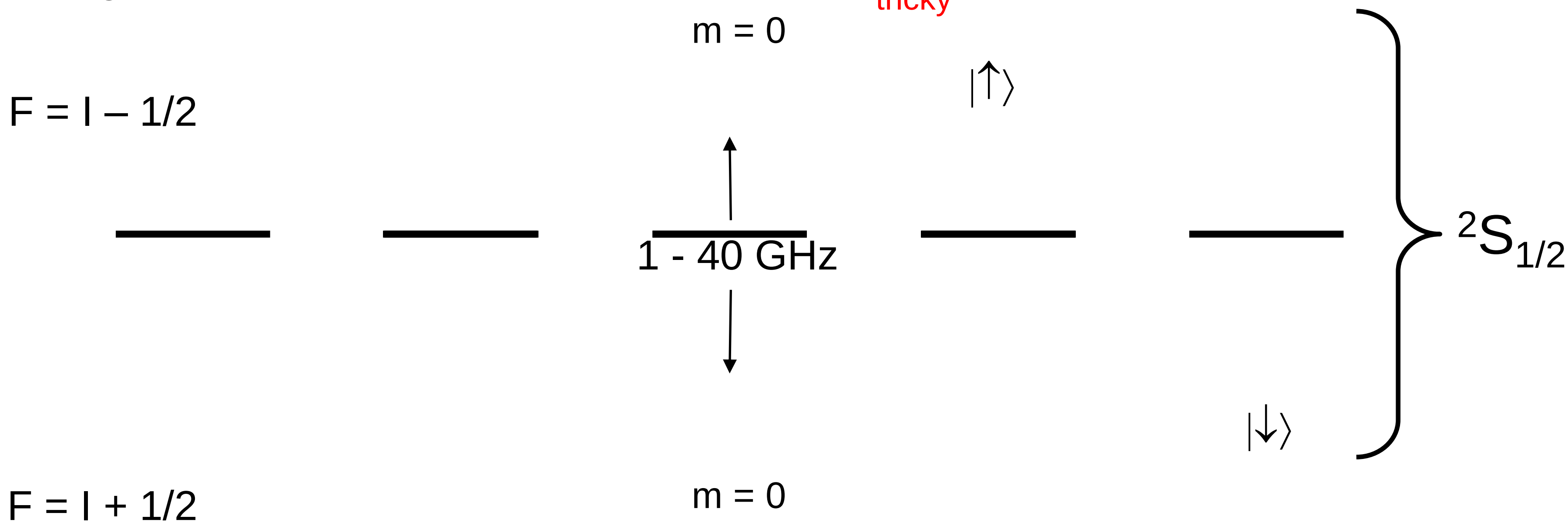

Optical qubit

$^2D_{5/2}$

Innsbruck/Weizmann

$|\uparrow\rangle$

with D

Ca^+	729 *nm*
Sr^+	674 *nm*
Ba^+	1760 *nm*
Yb^+	411 *nm*
Hg^+	282 *nm*

Advantages

- Single optical photon (momentum).
- B-field independent qubit (if nuclear spin ≠ 0).
- Hardly any spontaneous decay during gates.
- State selective fluorescence Detection: excellent discrimination.

Disadvantages

- Finite (~ 1 sec) $|\uparrow\rangle$ lifetime.
- Coherence time is limited by laser linewidth.

$^2S_{1/2}$

$|\downarrow\rangle$

Qubit Initialization

Zeeman qubit

-Optical pumping into a dark state.

-CPT possible into any superposition..

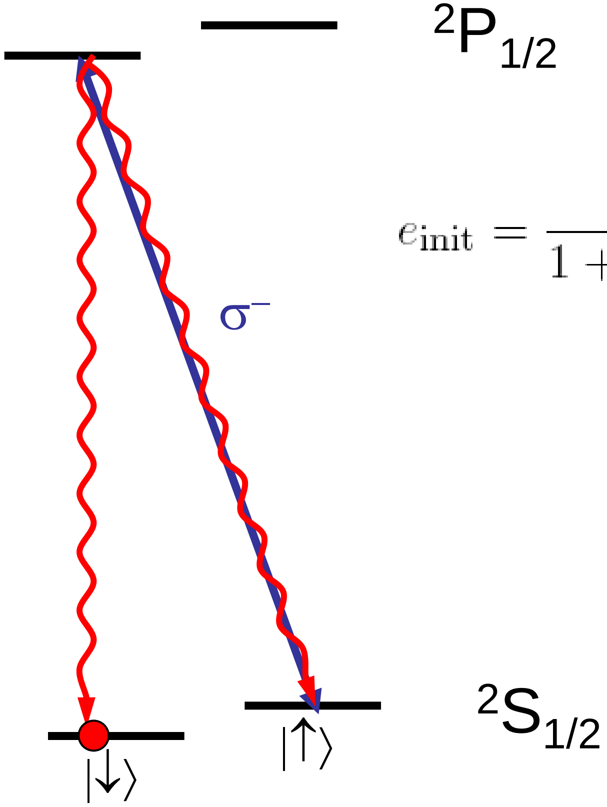

$$e_{\text{init}} = \frac{\epsilon_\pi}{1+\delta_\pi^2/\gamma'^2} + \frac{\epsilon_{\sigma^-}}{1+\delta_{\sigma^-}^2/\gamma'^2}$$

$$\gamma' = \frac{\gamma}{2}\sqrt{1+s_0}$$

$\varepsilon \sim 10^{-6} - 10^{-3}$

Error sources:
- Polarization purity.

Qubit Initialization

Zeeman qubit

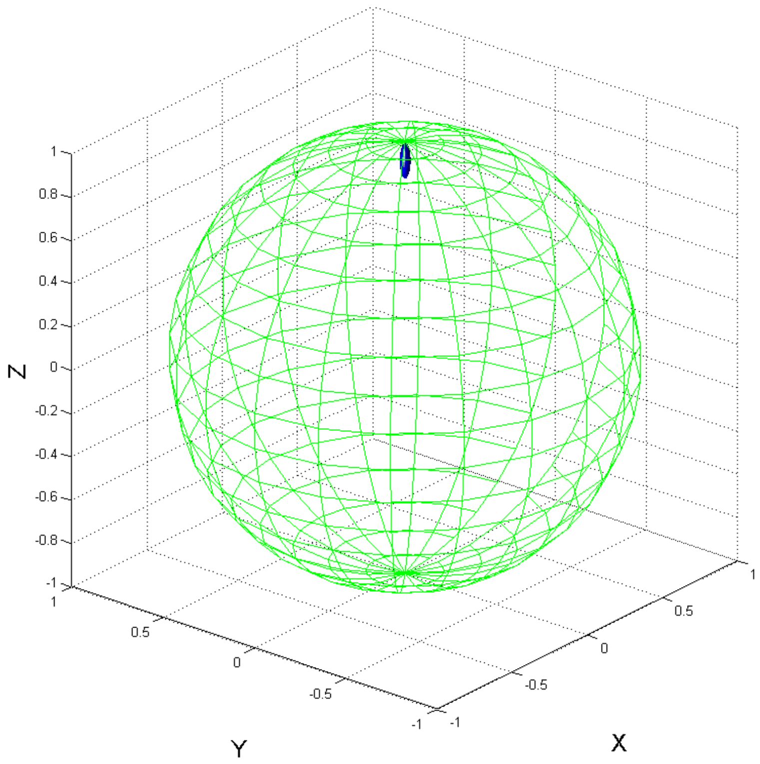

Process tomography of optical pumping

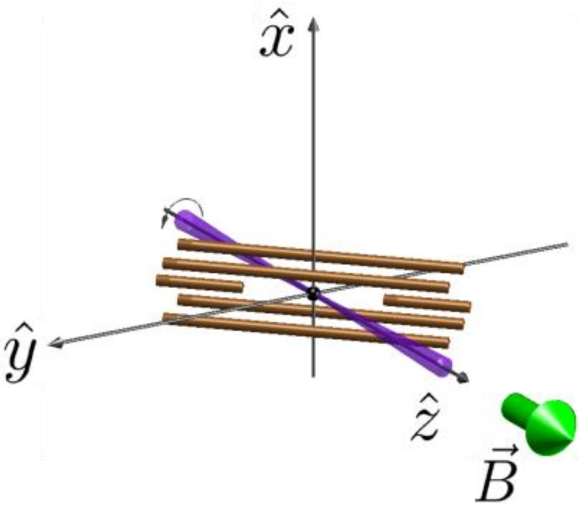

Limited to 10^{-3} due to stress-induced birefringence in vacum chamber optical viewports

Qubit Initialization

Zeeman qubit: the D level option

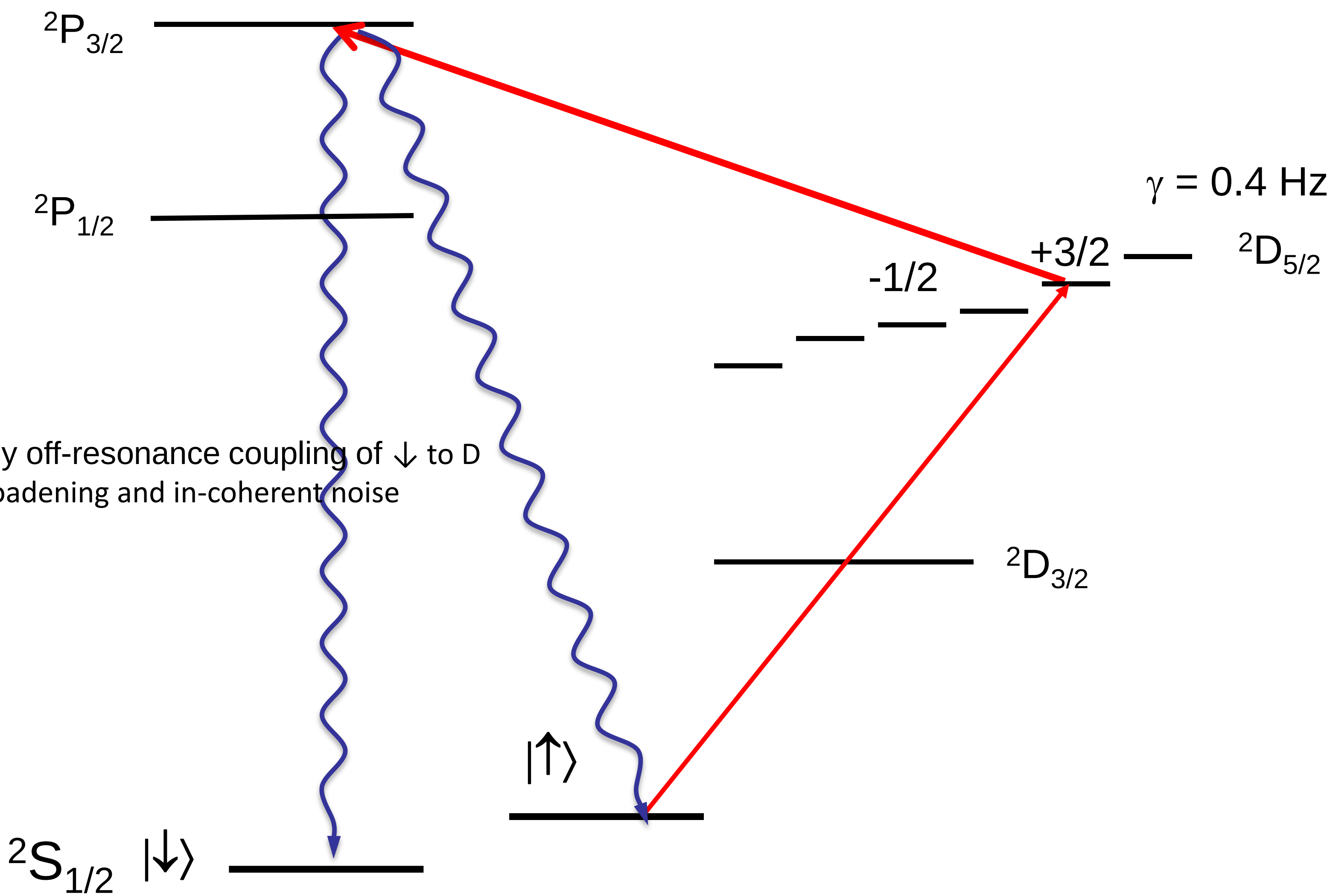

- Limited by off-resonance coupling of ↓ to D
- Power broadening and in-coherent noise
- $\varepsilon = 10^{-4}$

Keselman, Glickman, Akerman, Kotler and Ozeri, New J. of Phys. **13**, 073027, (2011)

Qubit Initialization

Hyperfine qubit

- Optical pumping into a dark state.

<u>Estimated:</u>

$$\epsilon \lesssim 2 \times 10^{-5}$$

C. Langer, Ph.D Thesis, University of Colorado, (2006).

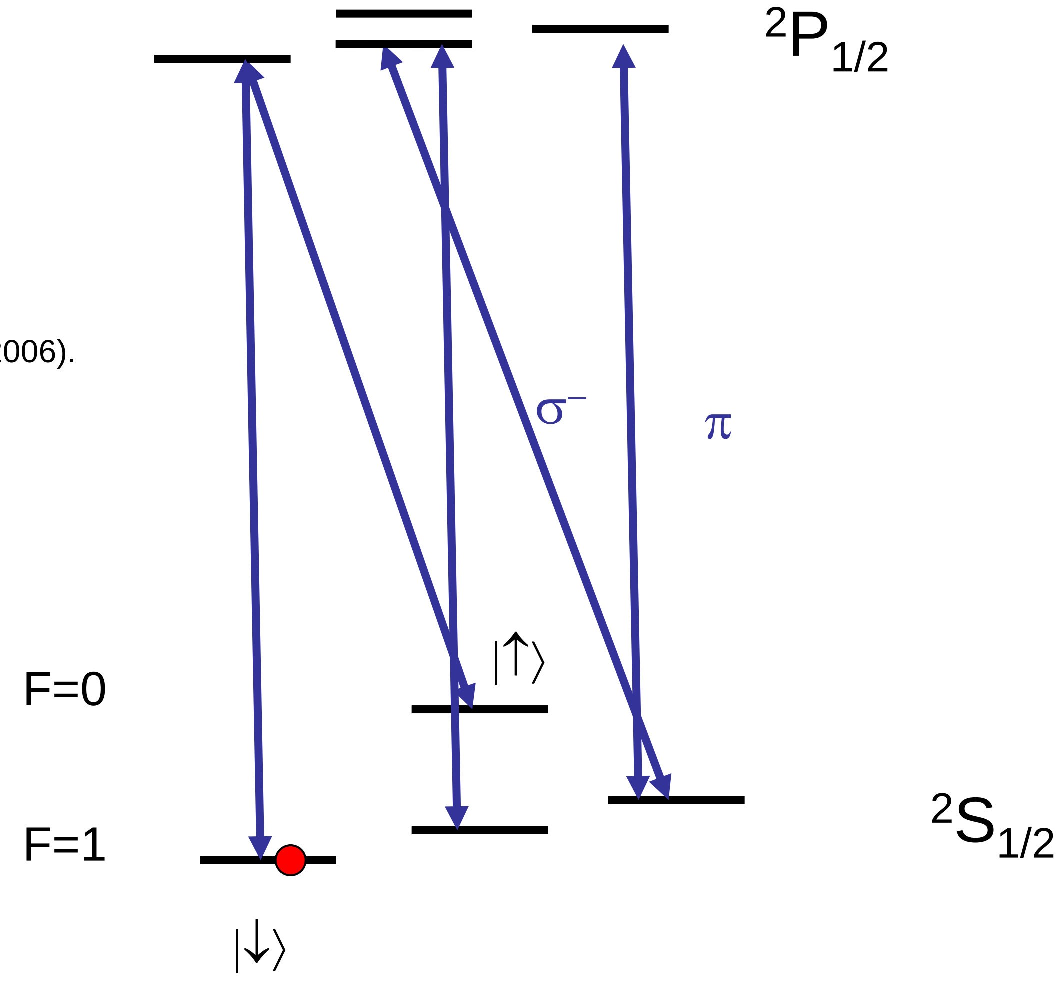

Qubit Initialization

Optical qubit

- $|\downarrow\rangle$ state initialization: same as previous.

- $|\uparrow\rangle$ state initialization:

  - Rapid adiabatic passage.

    $\varepsilon \sim 10^{-2}$

    (Wunderlich et. al. Journal of Modern Optics 54, 1541 (2007))

  - π-pulse.

    $\varepsilon \sim 10^{-2}$

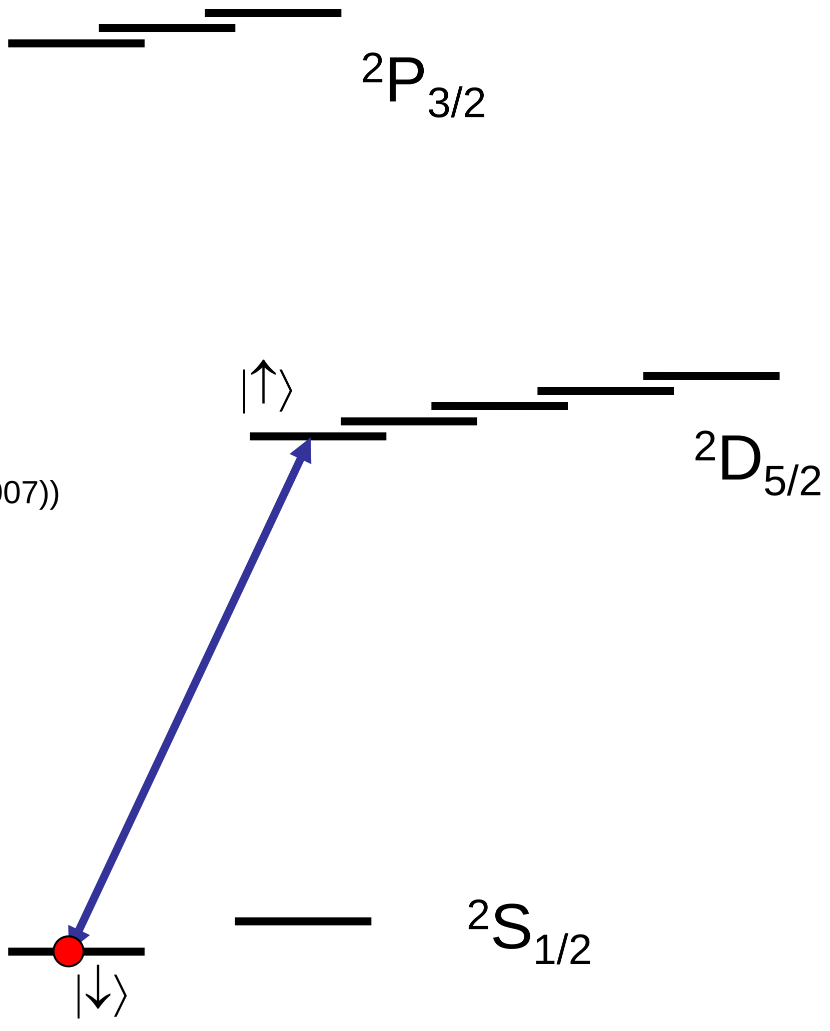

Measurement: state selective fluorescence

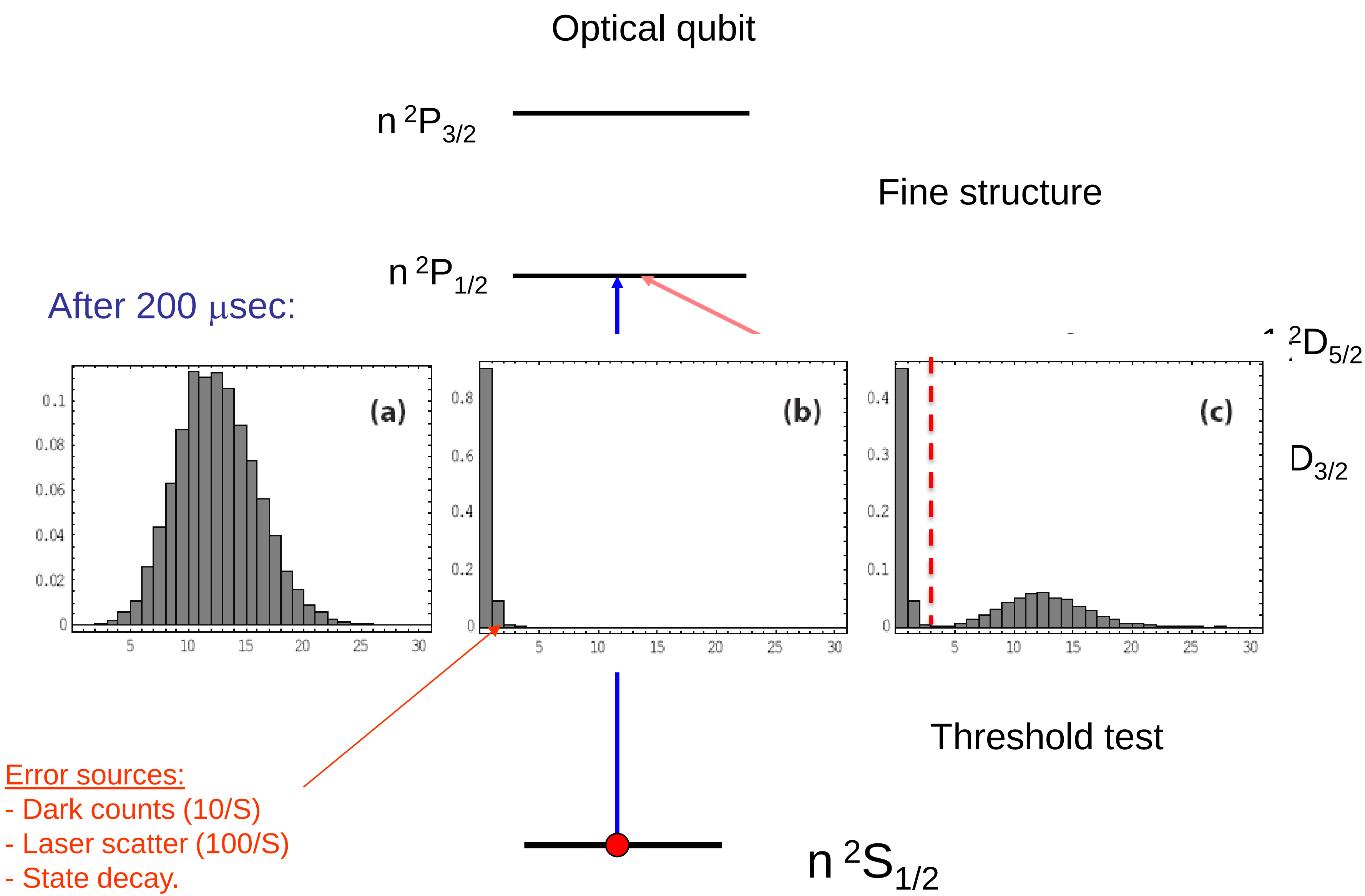

Zeeman Qubit Detection

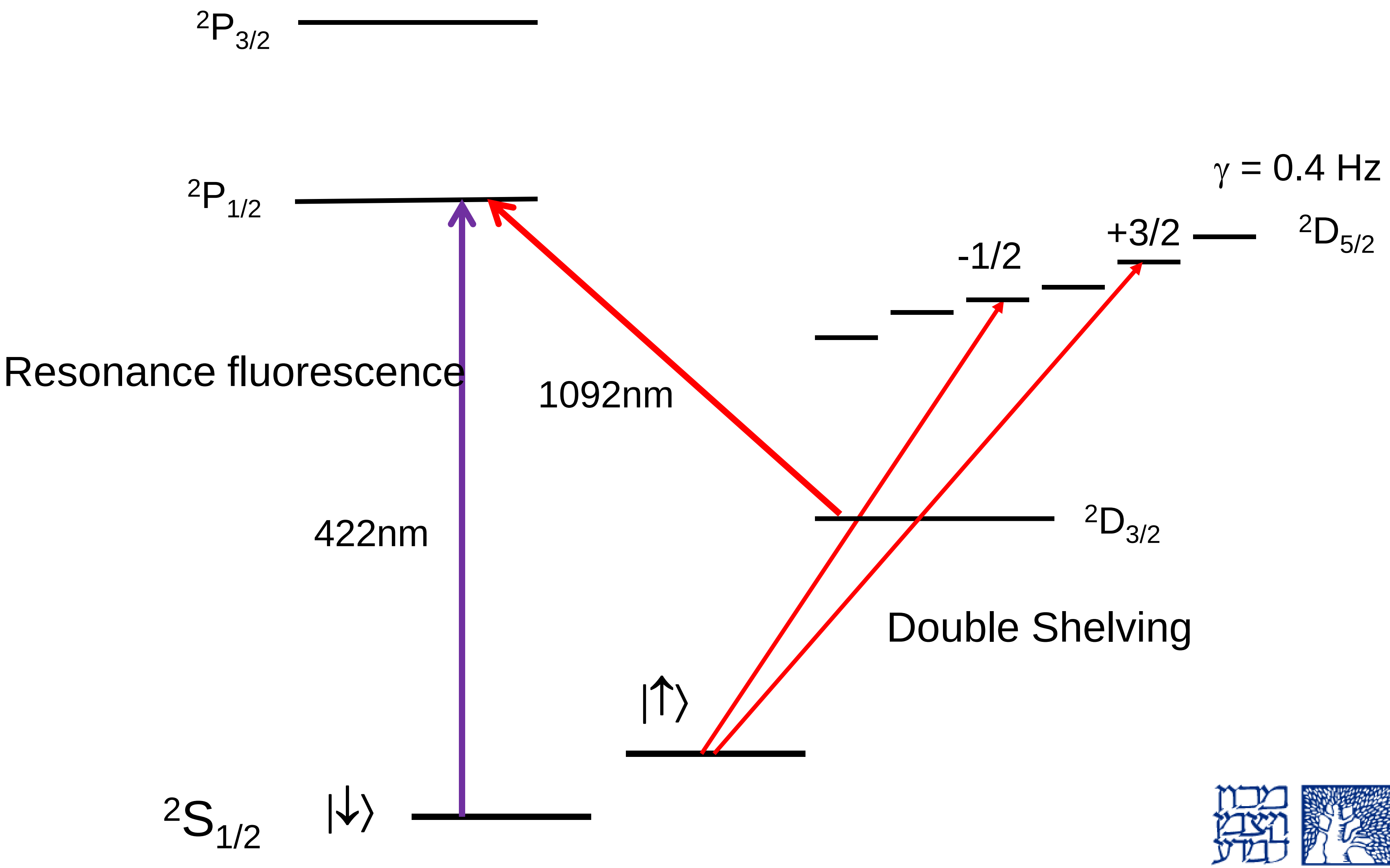

$^{88}Sr^{+}$ Zeeman Qubit Detection

Expected distributions:
Bright photon detection rate: 73.5 kHz
Dark photon detection rate: 1.75 kHz
D level lifetime: 390 ms
Detection time: 285 μs

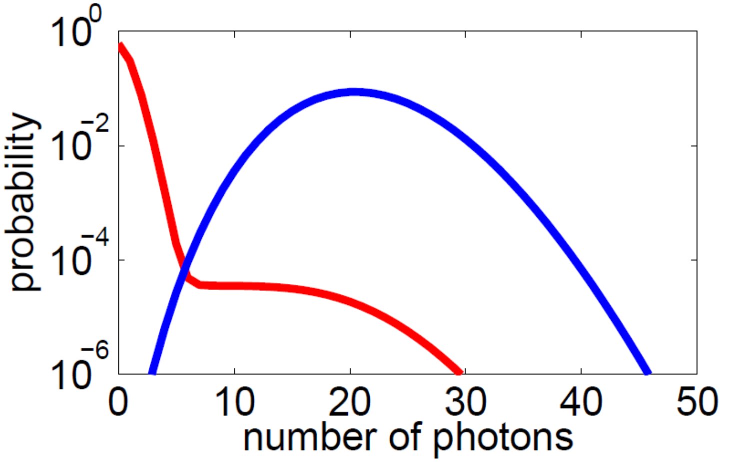

Measured for |↑>

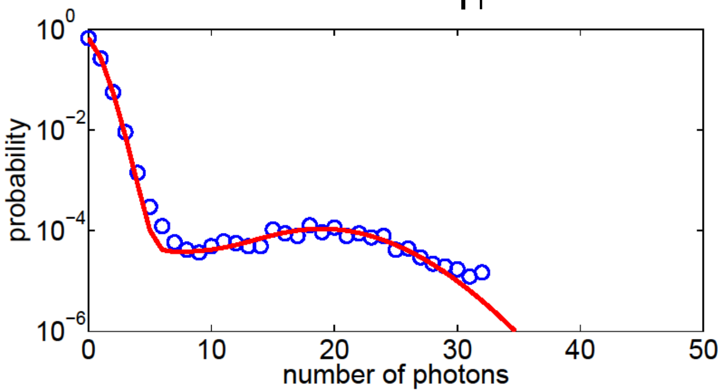

Measured for |↓>

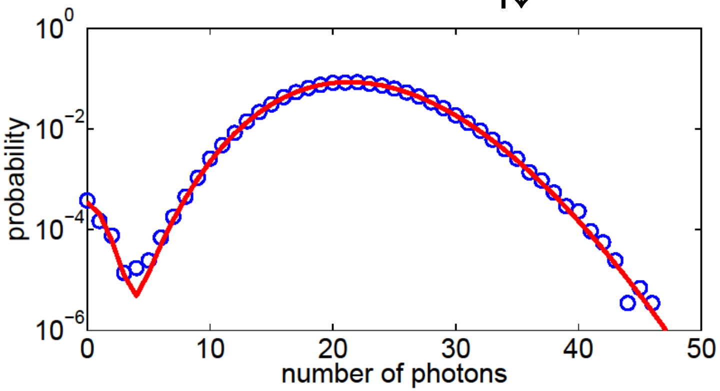

Initialization and shelving error: $\varepsilon_{\uparrow} = 1*10^{-3}$; $\varepsilon_{\downarrow} = 0.6*10^{-3}$

Keselman, Glickman, Akerman, Kotler and Ozeri, New J. of Phys. **13**, 073027, (2011)

$^{88}Sr^{+}$ Zeeman Qubit Detection

State discrimination error (10^{-4})

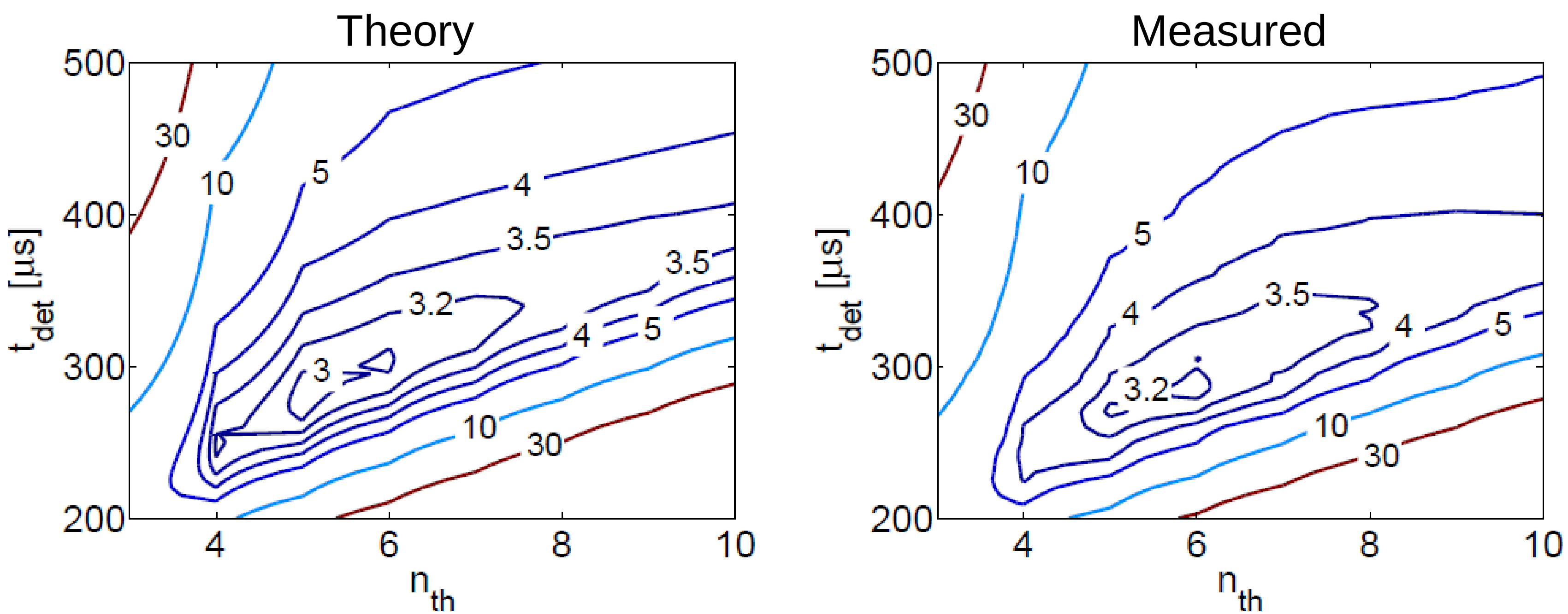

Minimal State discrimination error = 0.3*10^{-3} @ τ_{det}=285 μs and $n_{threshold}$=6

Average Detection fidelity: 0.9989

Keselman, Glickman, Akerman, Kotler and Ozeri, New J. of Phys. **13**, 073027, (2011)

Measurement: state selective fluorescence

Hyperfine qubit

Error Sources:
- Polarization purity (Bright->dark optical pumping).
- Off resonance dark->bright optical pumping.
- Dark counts (10/S).
- Laser scatter (100/S).

Benefit from:
- Large hyperfine splitting.
- Large angular momentum splitting between bright and dark states.

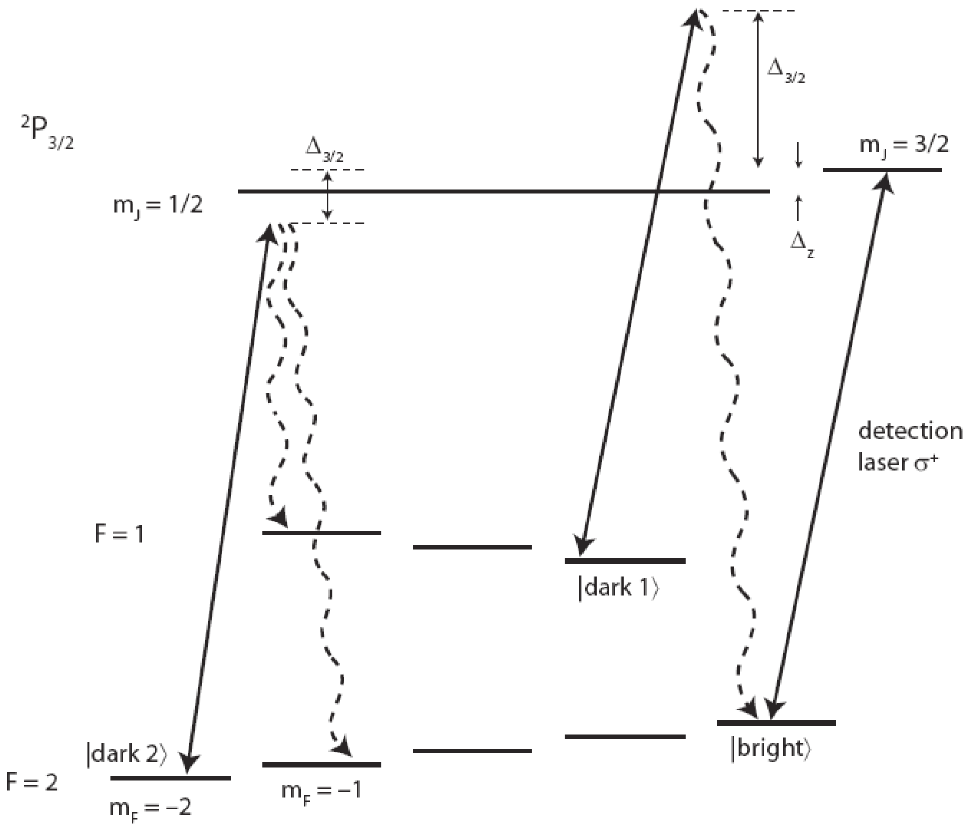

Threshold test: $\varepsilon \sim 8\times10^{-5}$

(C. Langer, Ph.D thesis, 2006) estimated, 200 μsec, no background

Measurement: Photon arrival time analysis

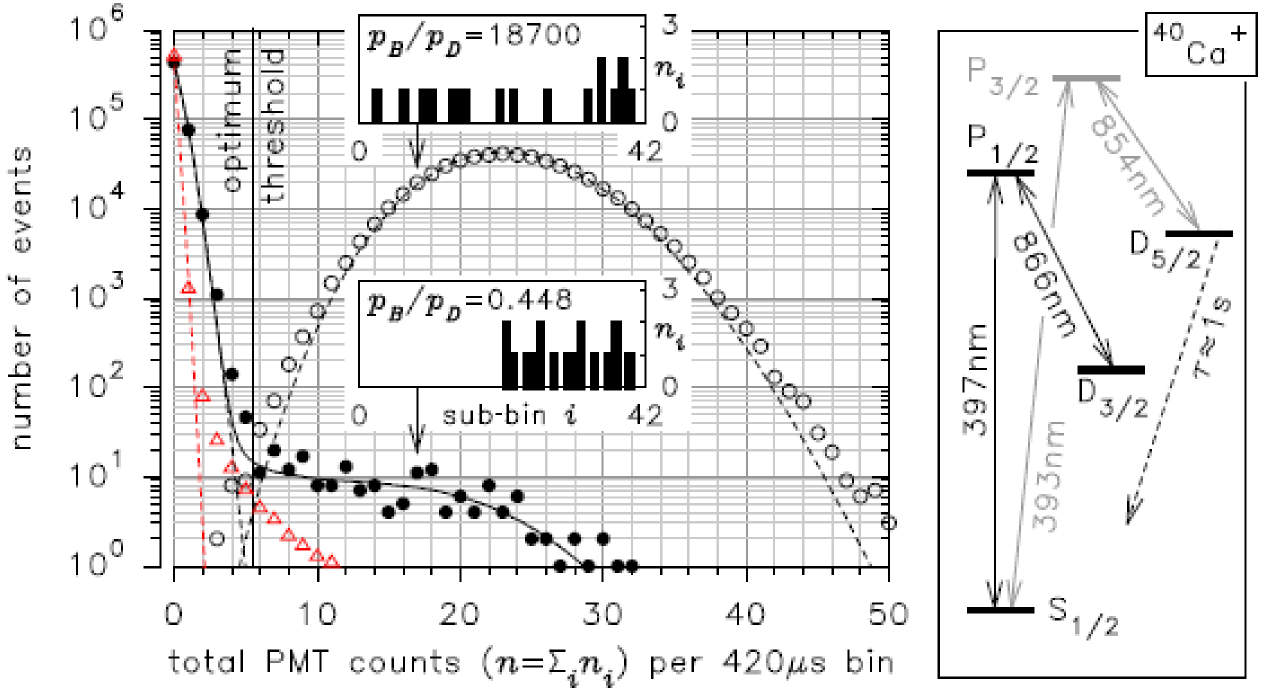

- Maximum likelihood test: $\varepsilon \sim 8.7\times10^{-5}$

(Myerson et. al. Phys. Rev. Lett. 100, 200502 (2008); Oxford ions)
225 μsec

(As compared with 1.8×10^{-4} threshold error in 420 μs)

Measurement with CCD

Antiferromagnetic ground-states in quantum magnetism (JQI, Maryland)

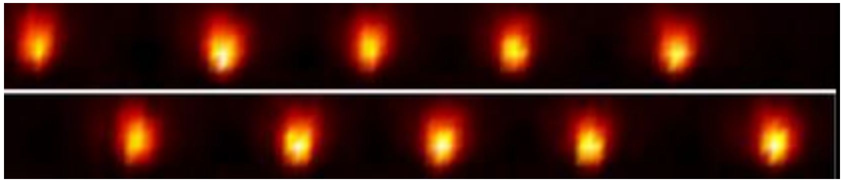

- Multiple ions: histograms overlap
- Which ion is bright?
- Slow readout
- Readout noise
- Cross-talk

Highest Camera fidelity (optical qubit; Oxford): 0.9991

Acton et. al. , Quant. Inf. Comp. 6, 465, (2006)

Burrell, Szwer, Webster and Lucas Phys. Rev. A 81, 040302, (2010)

Measurement: Other

- Photon detection efficiency:

  0.6 NA gives 0.99 in 10 μs and 0.9915 in 100 μs (hyperfine qubit, Duke)

  Noek et. al. arXiv1304.3511 (2013)

- Ancila qubits:

  • Entangled ancila for twice the fluoresence (hyperfine qubit; NIST)

    Schaetz et. al. PRL 94, 010501 (2005)

  • State transfer to a different species ion (optical qubit; NIST)

    Hume et. al. PRL 99, 137205 (2007)

Tutorial overview

1. The ion-qubit: different ion-qubit choices, Ion traps.

2. Qubit initialization.

3. Qubit measurement.

4. Universal set of quantum gates:
    single qubit rotations;
    two-ion entanglement gates

5. Memory coherence times

How well???

Benchmarked to current threshold estimates

Disclaimer: non exhaustive; focuses on laser-driven gates

Single qubit gates

Reviewed in many places e.g. :

- D. Wineland, *Les Houches lecture notes*. (2003).
- D. Wineland *et.al., J. Res. Natl. Inst. Stand. Technol*., **103**, 259, (1998).
- D. Leibfried *et. al*., *Rev. Mod. Phys*., **75**, 281, (2003).

- Coupling between the two qubit levels using e.m. traveling plane waves (far-field).

For a single ion: $$\hat{H}(t) = \hat{H}_0 + \hat{V}(t)$$

$\hat{H}_0 = \frac{1}{2}\hbar\omega_0\hat{\sigma}_z + \hbar\omega_m(\hat{a}^\dagger\hat{a} + \frac{1}{2})$ and $\hat{V}(t) = \hbar\Omega_0(\hat{\sigma}^+ + \hat{\sigma}^-)\cos(k\hat{x} - \omega t + \phi)$

Coupling strength

Where:

$$\hat{\sigma}_- = \hat{\sigma}_x + i\hat{\sigma}_y = |\downarrow\rangle\langle\uparrow|$$

$$\hat{\sigma}_+ = \hat{\sigma}_x - i\hat{\sigma}_y = |\uparrow\rangle\langle\downarrow|$$

$$x_0 = \sqrt{\frac{\hbar}{2M\omega_m}}$$

$$\boldsymbol{k}\hat{x} = kx_{\text{eq}} + kx_0(\hat{a}^\dagger + \hat{a}) \equiv kx_{\text{eq}} + \eta(\hat{a}^\dagger + \hat{a})$$

Typp. 0.05-0.2 for optical *k*

Single qubit gates

In the interaction representation and within the Rotating Wave Appr. (RWA)

$$H_{int}(t) = \hbar\Omega_0/2\hat{\sigma}_+ \exp(i\eta(\hat{a}e^{-i\omega_m t} + \hat{a}^\dagger e^{i\omega_m t}))e^{i(kx_{eq}+\phi-\delta t)} + H.C.$$

0

When $\delta = s\omega_m$, only $|\downarrow, n\rangle$ and $|\uparrow, n+s\rangle$ will be resonantly coupled (another RWA).

$$\Omega_{n,n+s} = \Omega_{n+s,n} = \Omega_0 |\langle n+s| e^{i\eta(\hat{a}+\hat{a}^\dagger)} |n\rangle| \equiv \Omega_0 D_{n+s,n}$$

$$D_{n+s,n} = \exp\left(-\eta^2/2\right)\eta^{|s|}\left(\frac{n_<!}{n_>!}\right)^{1/2} L_{n_<}^{|s|}\left(\eta^2\right)$$ Debye – Waller factor

Carrier: $s = 0$

$$\hat{H}_{\text{carrier}} = \frac{\hbar\Omega_{n,n}}{2}\left(\hat{\sigma}_+ \exp\left(i\phi\right) + \hat{\sigma}_- \exp\left(-i\phi\right)\right)$$

Red sideband (RSB): $s = -1$

$$\hat{H}_{\text{RSB}} = \frac{\hbar\Omega_{n-1,n}}{2}\left(\hat{a}\hat{\sigma}_+ \exp\left(i\phi\right) + \hat{a}^\dagger\hat{\sigma}_- \exp\left(-i\phi\right)\right)$$

Blue sideband (BSB): $s = +1$

$$\hat{H}_{\text{BSB}} = \hat{H}_{\text{int}} = \frac{\hbar\Omega_{n+1,n}}{2}\left(\hat{a}^\dagger\hat{\sigma}_+ \exp\left(i\phi\right) + \hat{a}\hat{\sigma}_- \exp\left(-i\phi\right)\right)$$

Lamb – Dicke regime

$$\eta\sqrt{\langle(\hat{a}^\dagger + \hat{a})^2\rangle} \ll 1$$

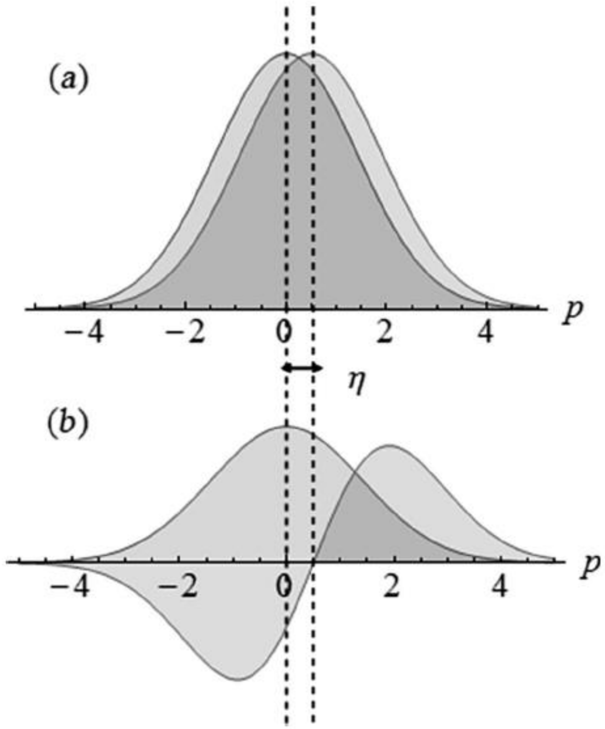

$$\Omega_{n,n} \simeq \Omega_0\left[1 - (n + 1/2)\eta^2\right],$$

$$\Omega_{n-1,n} \simeq \Omega_0 n^{1/2}\eta,$$

$$\Omega_{n+1,n} \simeq \Omega_0(n + 1)^{1/2}\eta.$$

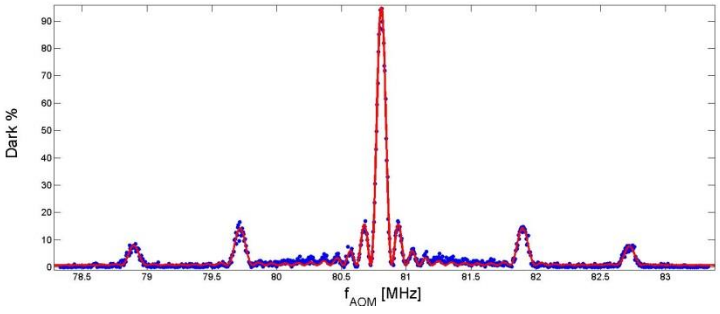

- Momentum conservation.

- Bosonic amplification.

Single qubit gates

Carrier rotations:

Since H_{int} is t independent:

$$|\psi(t)\rangle_{int} = e^{-i\hat{H}_{int}t/\hbar}|\psi(0)\rangle_{int} = e^{-i\theta\vec{\sigma}\cdot\vec{n}}|\psi(0)\rangle_{int} \equiv \hat{R}(\theta,\phi)|\psi(0)\rangle_{int}$$

$$\theta = \Omega_0 t \qquad\qquad \vec{n} = \begin{pmatrix} \cos(\phi) \\ i\sin(\phi) \\ 0 \end{pmatrix}$$

$$\hat{R}(0,\phi,\theta) = \begin{bmatrix} \cos(\theta/2) & -ie^{i\phi}\sin(\theta/2) \\ -ie^{-i\phi}\sin(\theta/2) & \cos(\theta/2) \end{bmatrix}$$

Coherent qubit (carrier) rotations

$$R(\theta, \phi)$$

$$R(\pi, 0)$$

$$R(\pi/2, \pi/2)$$

Bloch sphere

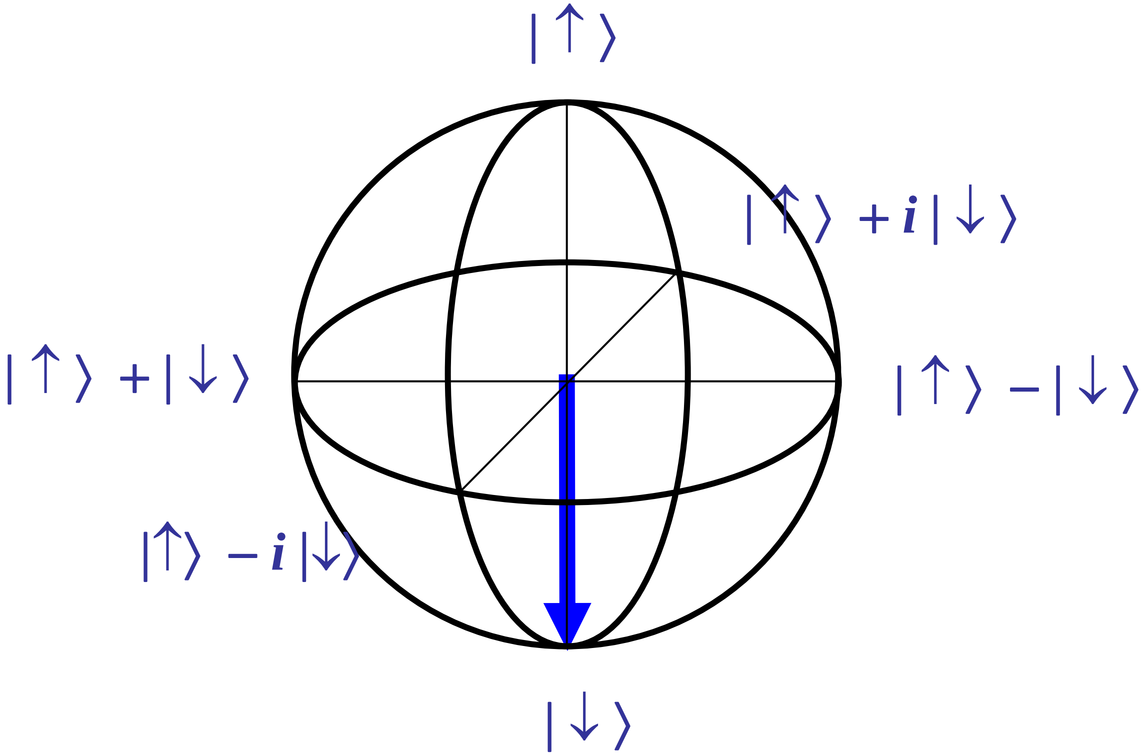

Any single qubit rotation can be composed of 1-3 pulses

Single qubit gates

RF qubit (Zeeman or Hyperfine)

Magnetic dipole coupling

$$V(t) = -\hat{\mu} \cdot B_0 \cos\left(\boldsymbol{k}\hat{x} - \omega t + \phi\right)$$

$$\hat{\mu} = \mu_B(g_S\hat{\mathbf{S}} + g_L\hat{\mathbf{L}} + g_I\hat{\mathbf{I}}) \quad \Rightarrow \quad \Omega_0 = \langle\downarrow|\hat{\mu} \cdot \mathbf{B_0}|\uparrow\rangle$$

e.g. for a Zeeman qubit:

$$\mathbf{B_0} = B_0\hat{\mathbf{x}}$$

$$\hat{\mu} = g_S\mu_B\hat{\sigma}$$

g_S ≈2 μ_B ≈1.4 MHz/G

$$\Omega_0 = 2\pi \times 2.8 B_0 \quad \text{MHz/G}$$

Advantages
- Very classical and controlled.

Disadvantages
- No momentum transfer ($\eta = 0$)
- No single qubit addressing.
  (… In the far field)

Single qubit gates

RF qubit (Zeeman or Hyperfine)

Magnetic dipole coupling

e.g. $^{88}Sr^{+}$ Zeeman qubit

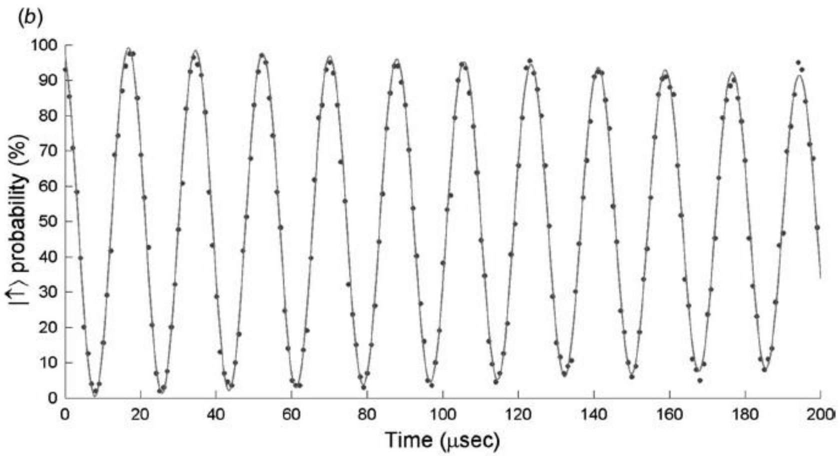

$\varepsilon = 2\times10^{-3}$

Error sources:

- Fluctuations in RF power.
- Relative phase/frequency noise (e.g. B field noise).

Process Tomography of the Identity operation

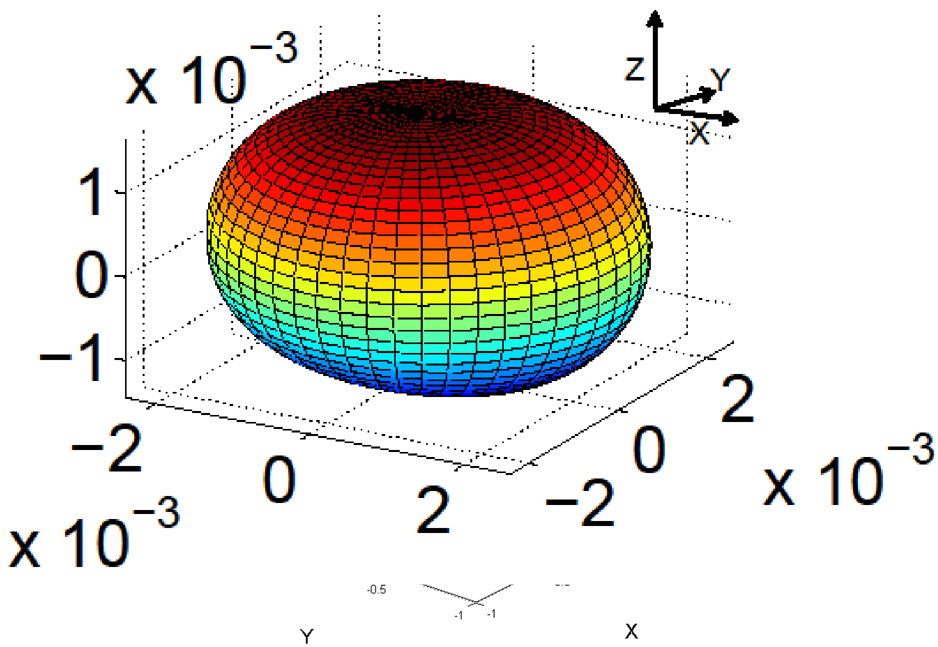

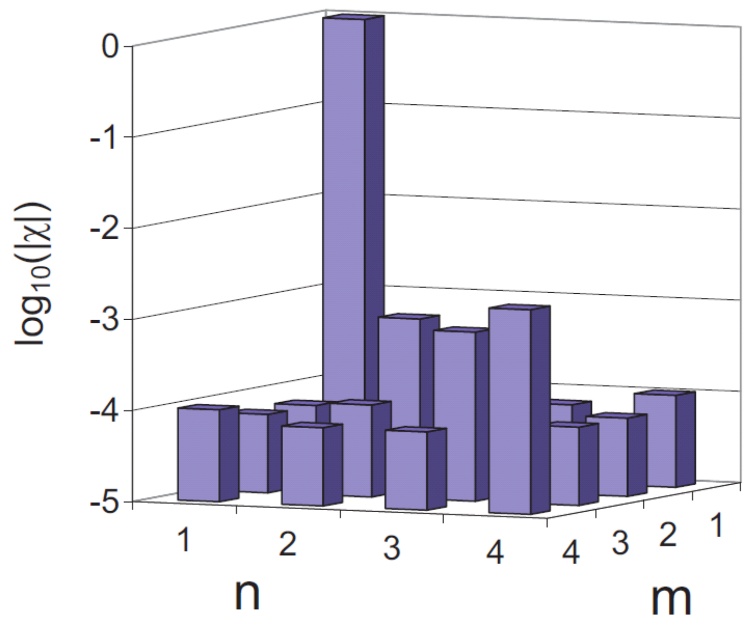

$E_1 = \hat{I},\ E_2 = \hat{\sigma}_x,\ E_3 = -i\hat{\sigma}_y,\ E_4 = \hat{\sigma}_z$

Process tomography Fidelity

$$F_{proc} = Tr(\chi_{ideal}\chi_{proc}) = 0.997(1)$$

Keselman, Glickman, Akerman, Kotler and Ozeri, New J. of Phys. **13**, 073027, (2011)

Single qubit gates

RF qubit (Zeeman or Hyperfine)

Two-photon Raman coupling

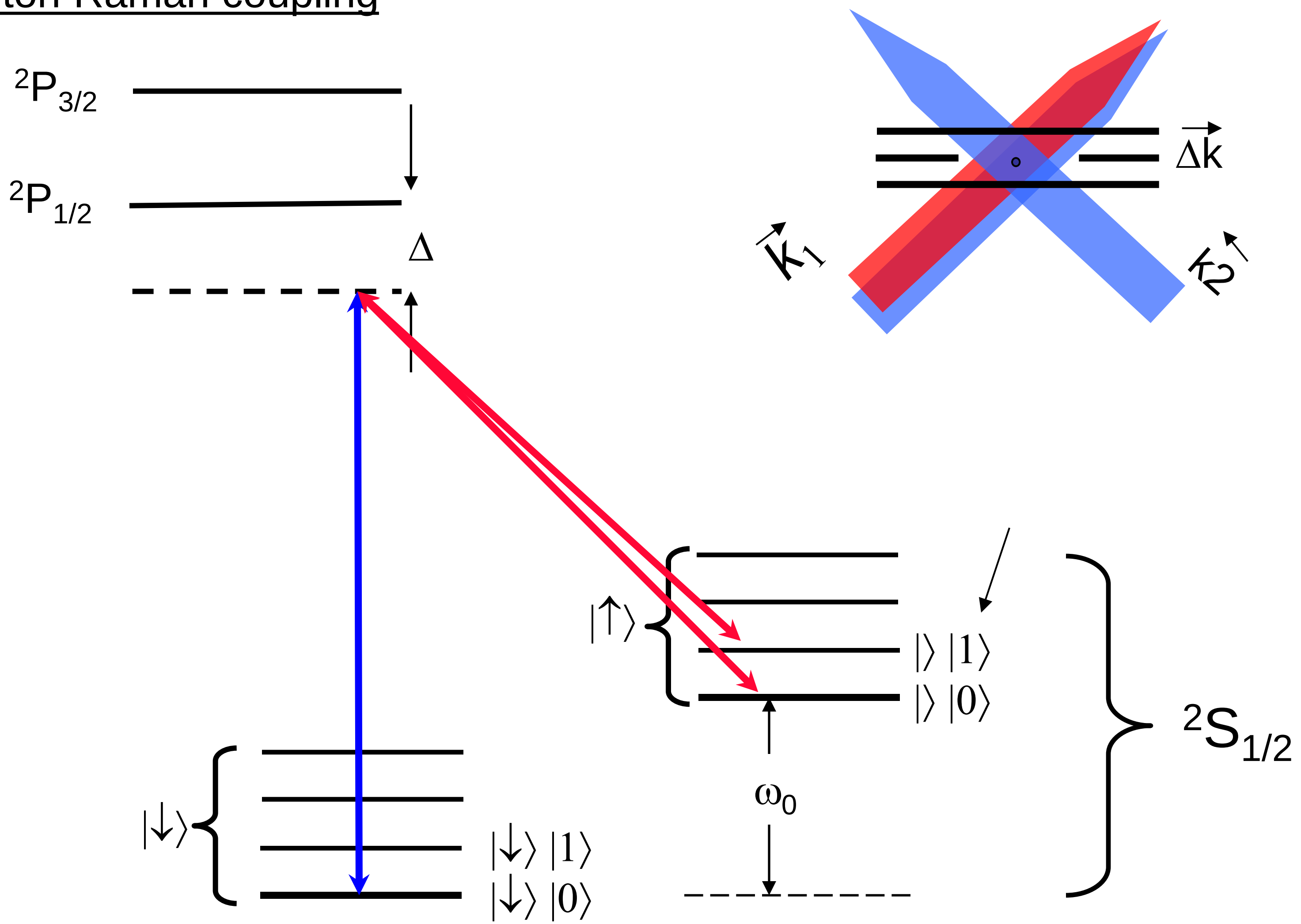

Single qubit gates

RF qubit (Zeeman or Hyperfine)

Two-photon Raman coupling

- Including the ^{2}P levels we have three (or more) level coupling.
- For large enough Δ excited states are "adiabatically eliminated".
- Back to "effective" two level coupling.

$$\vec{E}_r = \hat{\epsilon}_r E_{r0} \cos(\vec{k}_r \cdot \hat{x} - \omega_r t + \phi_r) \qquad \vec{E}_b = \hat{\epsilon}_b E_{b0} \cos(\vec{k}_b \cdot \hat{x} - \omega_b t + \phi_b)$$

For a single excited state:

$$\phi = \phi_b - \phi_r$$

$$\Omega_0 = \frac{E_{r0} E_{b0}}{4\hbar^2} \sum_i \frac{\langle \uparrow | \hat{\mathbf{d}} \cdot \vec{\epsilon_r} | e_i \rangle \langle e_i | \hat{\mathbf{d}} \cdot \vec{\epsilon_b} | \downarrow \rangle}{\Delta_i}$$

$$\vec{k} = \Delta\vec{k} = \vec{k}_b - \vec{k}_r$$

Single qubit Raman gates

Stark shifts

$$\hat{H}_{int} = \frac{\hbar\Omega_0}{2} D_{n,n}(\hat{\sigma}_+ e^{i\phi} + \hat{\sigma}_- e^{-i\phi}) + (\Delta_\uparrow - \Delta_\downarrow)\hat{\sigma}_z$$

$$\Delta_\uparrow = \frac{|E_r|^2}{4\hbar^2} \sum_i \frac{|\langle\uparrow|\hat{\mathbf{d}}\cdot\vec{\epsilon}_r|e_i\rangle|^2}{\Delta_{i,r}} + \frac{|E_b|^2}{4\hbar^2} \sum_i \frac{|\langle\uparrow|\hat{\mathbf{d}}\cdot\vec{\epsilon}_b|e_i\rangle|^2}{\Delta_{i,b}}$$

$$\Delta_\downarrow = \frac{|E_r|^2}{4\hbar^2} \sum_i \frac{|\langle\downarrow|\hat{\mathbf{d}}\cdot\vec{\epsilon}_r|e_i\rangle|^2}{\Delta_{i,r}} + \frac{|E_b|^2}{4\hbar^2} \sum_i \frac{|\langle\downarrow|\hat{\mathbf{d}}\cdot\vec{\epsilon}_b|e_i\rangle|^2}{\Delta_{i,b}}$$

- Differential Stark shift can be tuned to zero with beam polarizations and detuning.

Single qubit gates

RF qubit (Zeeman or Hyperfine)

Raman carrier transitions: co-propagating beams.

$^{9}Be^{+}$, $|F=1, mf = -1\rangle$; $|F=2, mf = -2\rangle$

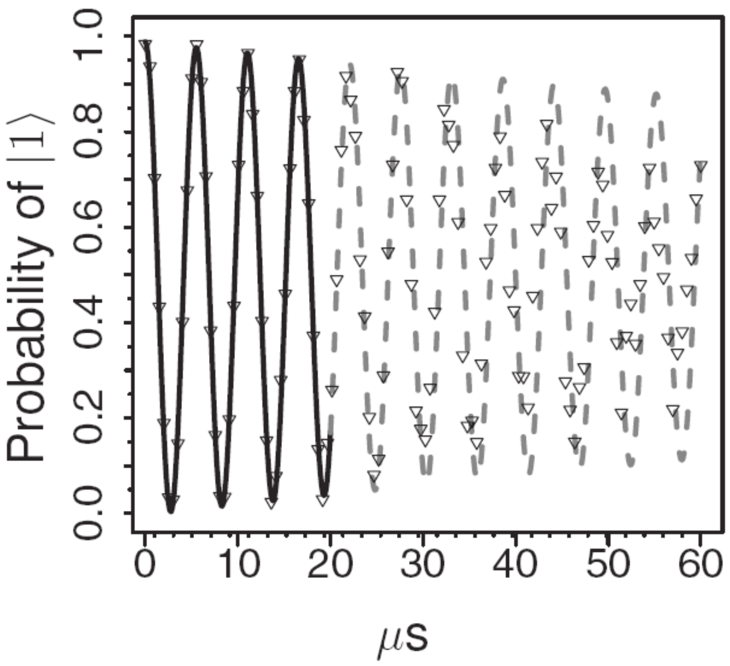

$^{43}Ca^{+}$, Clock transition

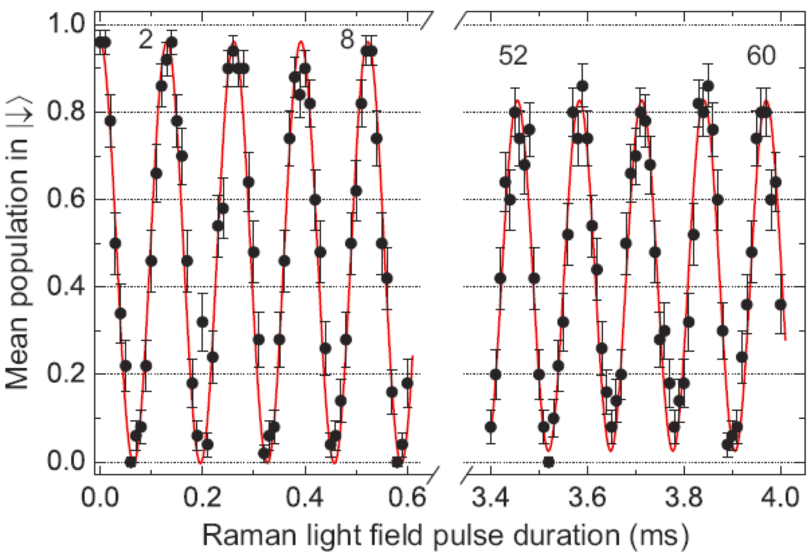

Knill *et. al*. *PRA*, **77**, 012307, (2008) (NIST Boulder)

Benhelm *et. al*. *quant-ph/0804.1261* (2008) (Innsbruck)

Single qubit gates

RF qubit (Zeeman or Hyperfine)

Two-photon Raman coupling

Randomizing gates:

ε in a $\pi/2$ gate = 0.0048

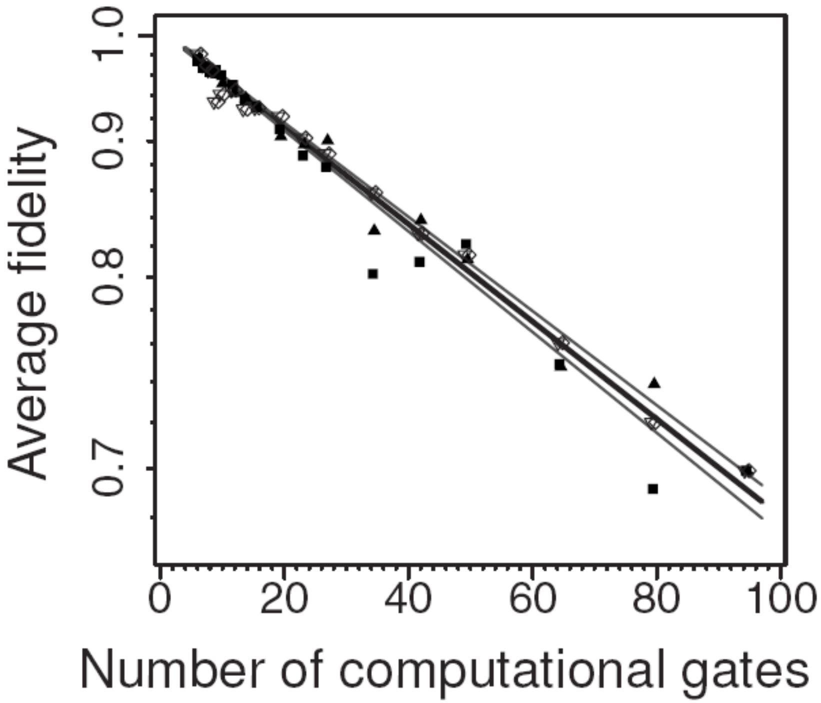

Error sources:
- Laser intensity and beam pointing noise.
- Inelastic spontaneous scattering of photons.
- B field noise.

Knill *et. al*. *PRA*, **77**, 012307, (2008) (NIST Boulder)

Single qubit gates

Optical qubit

Electric Quadruple coupling

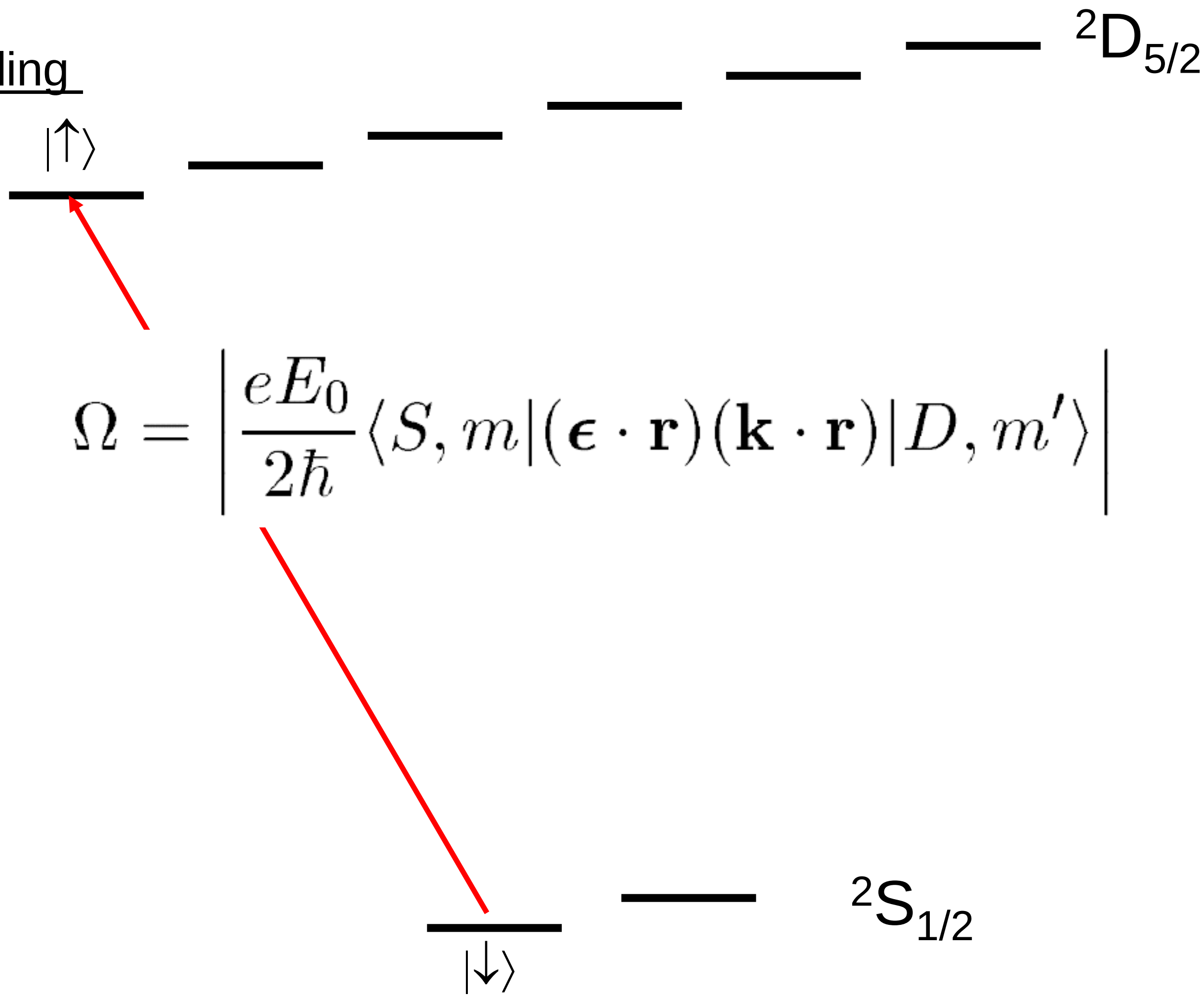

$$\Omega = \left| \frac{eE_0}{2\hbar} \langle S, m | (\boldsymbol{\epsilon} \cdot \mathbf{r})(\mathbf{k} \cdot \mathbf{r}) | D, m' \rangle \right|$$

Single qubit gates

<u>Optical qubit: Electric Quadruple coupling</u>

99 %

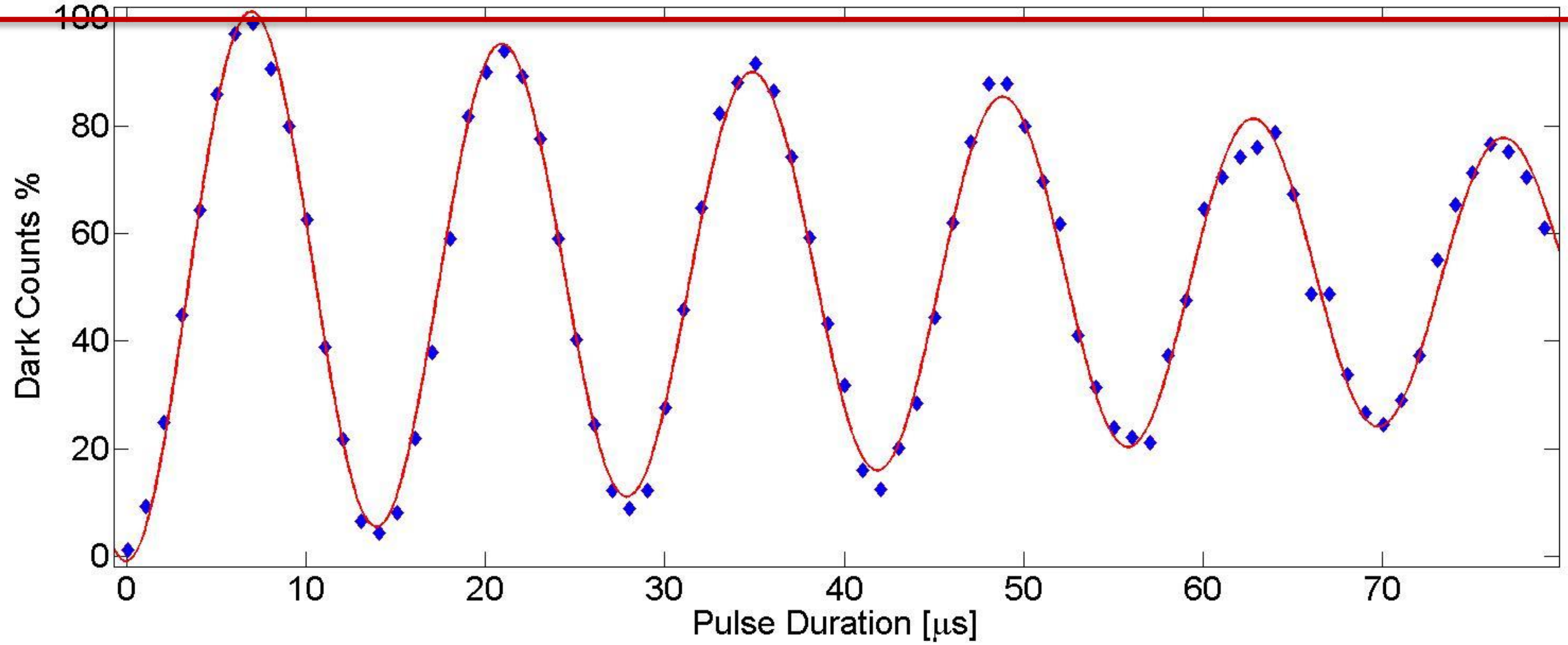

<u>Required:</u>

- Ground-state cooling
- Intensity noise-eater.
- Frequency auto-calibration every 100 s.

<u>Error sources:</u>

- Beam pointing~ 0.3%
- Frequency drift 0.3%
- Laser linewidth 0.2%.
- Magnetic field noise 0.1%.

Keselman, Glickman, Akerman, Kotler, & Roee Ozeri, New J. Phys.13 073027 (2011)

Single qubit gates: Individual addressing

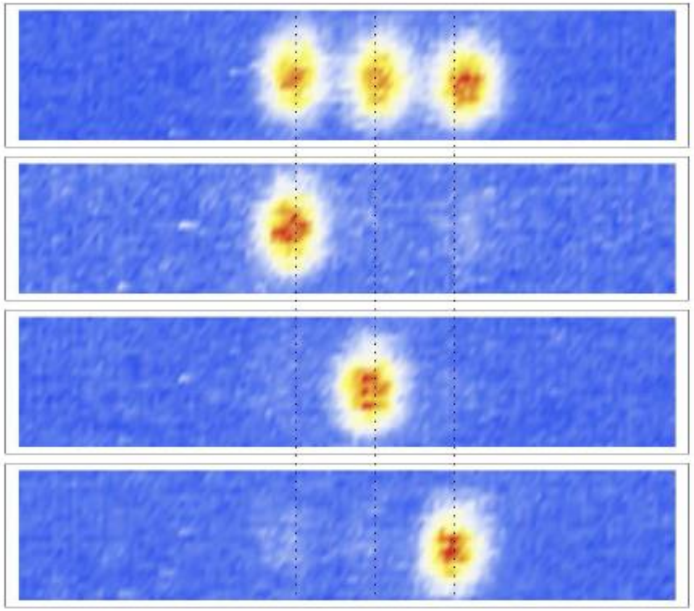

- Spatial: tightly focused laser beams (Innsbruck)
- Spatial: Large gradients in MW fields (NIST)
- Spectral: Large B field gradients (Siegen)
- Spectral: Inhomogeneous dressing field (Weizmann)